

Inverse Kinematics of Human Arm Based on Multisensor Data Integration

Matjaž Mihelj

Received: 23 May 2006 / Accepted: 29 August 2006 /
Published online: 30 September 2006
© Springer Science + Business Media B.V. 2006

Abstract The paper considers a technique for computation of the inverse kinematic model of the human arm. The approach is based on measurements of the hand position and orientation as well as acceleration and angular rate of the upper arm segment. A quaternion description of orientation is used to avoid singularities in representations with Euler angles. A Kalman filter is designed to integrate sensory data from three different types of sensors. The algorithm enables estimation of human arm posture, which can be used in trajectory planning for rehabilitation robots, evaluation of motion of patients with movement disorders, and generation of virtual reality environments.

Key words Kalman filter · kinematics · man–machine systems · quaternion · sensor integration

1 Introduction

Upper-limb orthotic systems have been designed for restoring the upper limb functions in individuals with disabilities resulting from spinal cord injury (SCI), stroke and muscle dystrophy. These systems are based either on functional electrical stimulation (FES) or rehabilitation robots and haptic interfaces [1].

In rehabilitation the kinematic analysis of limb movements, which can be used to assess disability of patients with movement disorders, becomes an important issue. In this regard becomes relevant to measure not only the endpoint position of the arm, but also the respective joint angles. Moreover, when applying electrical stimulation to the upper-limb it is important to be aware of the arm configuration to properly select

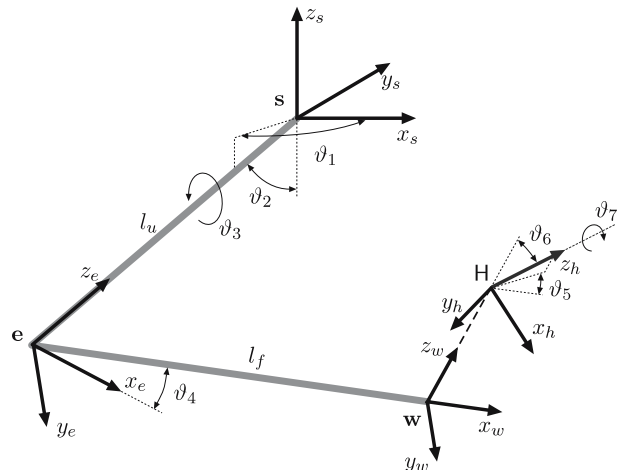
M. Mihelj (✉)
Faculty of Electrical Engineering, University of Ljubljana, Tržaška c. 25,
SI-1000 Ljubljana, Slovenia
e-mail: matjaz.mihelj@robo.fe.uni-lj.si

the required stimulation pattern. Therefore, it is necessary to calculate the inverse kinematics of the limb.

The human arm can be modeled as a seven-degree-of-freedom mechanism (Figure 1) consisting of the shoulder ball-and-socket joint, the elbow revolute joint, and the wrist ball-and-socket joint (for a more detailed kinematic model of the human arm see Lenarčič and Klopčar [2]). The shoulder and elbow joints are connected through the upper arm segment with the length l_u , and the elbow and the wrist joints through the forearm segment with the length l_f . The inverse kinematics problem of the human arm can be stated as follows: given the position and the orientation of the hand, find the seven joint angles. Since the given position and the orientation of the hand specify six, rather than seven, independent quantities, the arm is a redundant system, and there are an infinite number of solutions for the joint angles.

Several inverse kinematics algorithms have been proposed specifically for the human arm. Korein [3] observed that the first two shoulder joints along with their joint limits restrict the tip of the elbow to lie on a spherical polygon. By intersecting the elbow swivel circle with the polygon it is possible to determine the legal elbow configurations as a function of the joint limits of the first two joints. Tolani and Badler [4] proposed a strategy to reduce the degrees-of-freedom of the arm by one, so that it is possible to obtain the closed-form equations that solve the inverse kinematics. The reduction of the degrees-of-freedom is done by fixing one joint angle at its previous value. An inverse kinematics approach developed by Koga et al. [5] focuses on generating natural looking arm postures. They use the sensorimotor transformation model proposed by Soechting and Flanders [6] to guess a posture for the arm that matches physiological observations of humans. Because the solutions are not exact, the wrist position of the guessed posture may not be what is desired. Therefore, a pseudoinverse Jacobian iteration procedure has to be carried out to tune the joint angles till the correct wrist position is obtained. Loftin et al. [7] proposed an algorithm which incorporates the physiological observation that arm and hand postures are, for the most part, independent of each other into the inverse

Figure 1 Simplified kinematic model of the human arm with 7 degrees of freedom; l_u and l_f are the upper arm and the forearm lengths respectively; s , e , and w indicate shoulder, wrist and elbow positions respectively; H is the hand pose matrix.



kinematics problem to produce natural looking arm postures without invoking the pseudoinverse Jacobian iterations [7]. This means that it is possible to find the forearm and upper arm posture to match the wrist position and then determine the joint angles for the wrist to match the hand orientation. The arm posture is as in [5] determined by a simple sensorimotor transformation model.

The proposed algorithms give rather inaccurate estimates of the arm posture, which are good enough for graphical presentation and not suitable for use in control systems. In order to be able to adequately measure arm angles a position measurement system is required in addition to the mechanism of the rehabilitation robot or haptic device. These can either be complex optical or magnetic measurement systems or a more simple system consisting of flexible goniometers, which are less reliable and more cumbersome. On the other hand, with the use of a rehabilitation robot or haptic device, the position and orientation of the fixation of the mechanism to the human arm is already known from the kinematic model of the device. Therefore, it becomes reasonable to use these existent data with minimal additional measurements to cope with redundant degrees of freedom of the upper extremity.

Owing to the availability of low cost accelerometers and angular rate sensors it becomes reasonable to construct an inertial measurement system to enable computation of human arm posture. This paper considers development of an algorithm that uses the hand pose data and the inertial sensor output as inputs for the estimation process. Human body tracking using inertial sensors requires an attitude estimation filter capable of tracking in all orientations.

Finite rotations in space are described by 3×3 rotational transformation matrices, and these matrices can be specified by a set of three to nine parameters. Commonly used parameter triples for finite rotations include Euler angles, Cardan angles, and Rodrigues parameters. Four parameters are Euler axis and angle, Euler parameters (or quaternion formulation), and Cayley–Klein parameters. A parametrization that complements Euler angles and Euler parameters was proposed by Tsiotras and Longuski [8]. Directly using direction cosines for describing rotations requires a total of nine parameters with six constraints. For comparison of rotation parameters we refer the interested reader to survey papers by Spring [9] and Shuster [10]. Among all the representations for finite rotations only those of four parameters behave well for arbitrary rotations because a nonsingular mapping between parameters and their corresponding rotational transformation requires a set of four parameters at least [11]. The advantages and disadvantages of these alternative descriptions for the rotational kinematics vary with the particular application. The quaternion description was chosen here because of its frequent use in analysis of inertial measurement systems [12–14] as well as in the control of robot manipulators [15]. Using the quaternion formulation a mechanical system that involves rotation between various coordinate systems does not degenerate for any angular orientation and physical quantities pertaining to the motion of rotation such as angular displacement, velocity, acceleration, and momentum are derived in a simple manner [11]. A drawback of using the quaternion formulation together with statistical analysis of rotational data is analyzed in [16]. The solution is proposed in terms of optimal statistical operators for 3-dimensional rotational data.

Data generated by the robot position sensors, accelerometers and gyroscopes are integrated using an extended Kalman filter to obtain reliable arm posture estimates.

2 Methods

2.1 Direct Kinematic Model of the Human Arm

The kinematic chain of our interest contains seven joint variables, therefore it has one redundant degree of freedom. A simple physical interpretation of the redundant degree of freedom is based on the observation that if the wrist is held fixed, the elbow is still free to swivel about a circular arc whose normal vector is parallel to the straight line connecting the shoulder and the wrist [17].

In Figure 1, abbreviations **s**, **e** and **w** define positions of shoulder, elbow, and wrist joints relative to the base coordinate frame. Based on relations in Figure 1, the following arm transformation matrices can be defined

$$T_s = rot(z_s, \vartheta_1)rot(x_s, \vartheta_2)rot(z_s, \vartheta_3)tr(z_s, -l_u) \tag{1}$$

$$T_e = rot\left(z_e, \frac{\pi}{2}\right)rot(x_e, \vartheta_4)rot\left(z_e, -\frac{\pi}{2}\right)tr(x_e, l_f) \tag{2}$$

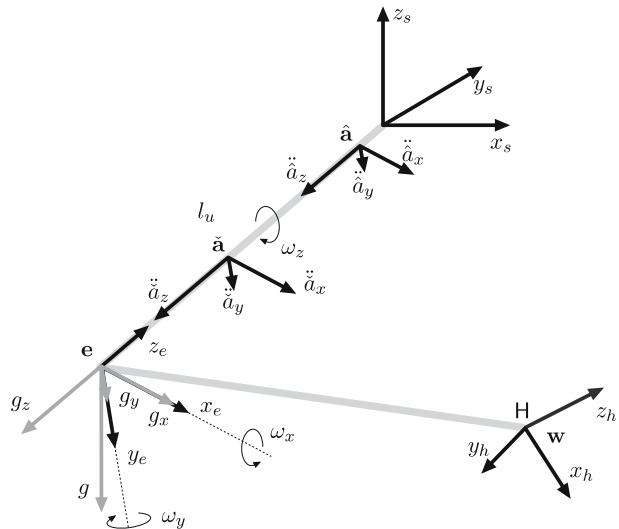
$$T_w = rot(z_w, \vartheta_5)rot(x_w, \vartheta_6)rot(z_w, \vartheta_7), \tag{3}$$

where *rot()* indicates rotation and *tr()* translation. T_s , T_e , and T_w are the shoulder, elbow, and wrist transformation matrices, respectively. Orientation is defined in terms of *zxz* Euler angles.

2.2 Measured Data

Figure 2 shows measurements available for the estimation process. The hand pose is constrained through the fixation of the hand to the robotic device – the hand is tightly coupled to the robot end-effector, forcing it to move jointly with the robot. The position and orientation of the hand, **H** (measured at the wrist position **w**), is computed from the robot direct kinematic model. Namely, robot joint angles are

Figure 2 Available measurements: hand pose **H** with wrist position **w**, upper arm angular rate $\Omega = [\omega_x \ \omega_y \ \omega_z]^T$, accelerations $\hat{\mathbf{a}} = [\hat{a}_x \ \hat{a}_y \ \hat{a}_z]^T$ at point $\hat{\mathbf{a}}$ and (optional measurement) $\check{\mathbf{a}} = [\check{a}_x \ \check{a}_y \ \check{a}_z]^T$ at point $\check{\mathbf{a}}$ on the upper arm.



always measured and if the robot reference coordinate frame is assumed as the general task reference frame, the hand pose matrix \mathbf{H} is directly available. If the task reference frame differs from the robot reference coordinate frame, the appropriate transformation matrix between the two frames needs to be applied. In addition to the hand pose matrix acceleration and angular rate of the upper arm are measured using a triad of accelerometers and a triad of gyroscopes. Placement of angular rate sensors is relatively simple, since their output is independent of their position. On the other hand, accelerometer output signal strongly depends on its position. Therefore, a careful analysis is required.

If the position of the shoulder joint is fixed and we assume the attachment point of the accelerometer close to the straight line connecting shoulder and elbow joints, is the measured acceleration at a point $\hat{\mathbf{a}} = [\hat{a}_x \hat{a}_y \hat{a}_z]^T$ (see Figure 2)

$$\ddot{\hat{\mathbf{a}}} = \begin{bmatrix} g s_2 s_3 + L_{\hat{a}} \left(\left(\frac{1}{2} \dot{\vartheta}_1^2 s_{22} - \ddot{\vartheta}_2 \right) s_3 + (2 \dot{\vartheta}_1 \dot{\vartheta}_2 c_2 + \ddot{\vartheta}_1 s_2) c_3 \right) \\ g s_2 c_3 + L_{\hat{a}} \left(\left(\frac{1}{2} \dot{\vartheta}_1^2 s_{22} - \ddot{\vartheta}_2 \right) c_3 - (2 \dot{\vartheta}_1 \dot{\vartheta}_2 c_2 + \ddot{\vartheta}_1 s_2) s_3 \right) \\ g c_2 - L_{\hat{a}} \left(\dot{\vartheta}_1^2 s_2^2 + \dot{\vartheta}_2^2 \right) \end{bmatrix} \tag{4}$$

where $L_{\hat{a}} = (\|\mathbf{e} - \hat{\mathbf{a}}\| - l_u)$, $c_2 = \cos \vartheta_2$, $c_3 = \cos \vartheta_3$, $s_2 = \sin \vartheta_2$, $s_3 = \sin \vartheta_3$ and $s_{22} = \sin(2\vartheta_2)$. Equation 4 shows that the acceleration at point $\hat{\mathbf{a}}$ consists of the gravity component that is independent of the accelerometer position and a dynamic component that depends on the distance between the elbow joint position and the accelerometer attachment point. In a point where $\|\mathbf{e} - \hat{\mathbf{a}}\|$ equals l_u the dynamic component vanishes. However, in this case it is required that the accelerometer be positioned exactly over the shoulder joint, what is relatively impracticable. When considering only slow movements the dynamic component of the measured acceleration $\ddot{\hat{\mathbf{a}}}$ can be neglected. On the other hand, when also fast movements have to be considered, an additional accelerometer can be used for measuring the acceleration of the upper arm in a second point at the location $\check{\mathbf{a}} = [\check{a}_x \check{a}_y \check{a}_z]^T$ [18, 19]. The acceleration $\check{\check{\mathbf{a}}}$ can be computed from Eq. 4 with $L_{\check{\check{\mathbf{a}}}} = (\|\mathbf{e} - \check{\check{\mathbf{a}}}\| - l_u)$.

With a simple algebraic manipulation, it is possible to eliminate acceleration dynamic components to obtain

$$\mathbf{g} = \begin{bmatrix} g_x \\ g_y \\ g_z \end{bmatrix} = \frac{L_{\hat{a}} \check{\check{\mathbf{a}}} - L_{\check{\check{\mathbf{a}}}} \ddot{\hat{\mathbf{a}}}}{L_{\hat{a}} - L_{\check{\check{\mathbf{a}}}}} = g \begin{bmatrix} \sin \vartheta_2 \sin \vartheta_3 \\ \sin \vartheta_2 \cos \vartheta_3 \\ \cos \vartheta_2 \end{bmatrix}. \tag{5}$$

2.3 Quaternion Algebra

A quaternion may be used to rotate a 3-dimensional vector \mathbf{u} using quaternion multiplications

$$\mathbf{u}_{rot} = Q^* \otimes \mathbf{u} \otimes Q, \tag{6}$$

where the quaternion $Q = [q_0 \ q_1 \ q_2 \ q_3]$ is defined as

$$Q = \cos \frac{\theta}{2} + \mathbf{r} \sin \frac{\theta}{2}, \tag{7}$$

with θ being the angle that the vector \mathbf{u} is to be rotated and \mathbf{r} being a unit vector that defines the axis of rotation. Q^* is the quaternion conjugate. Equation 6 can be rewritten in terms of rotation matrix as

$$\mathbf{u}_{rot} = M(Q)\mathbf{u}, \tag{8}$$

where

$$M(Q) = \frac{1}{\|Q\|} \begin{bmatrix} 1 - 2(q_2^2 + q_3^2) & 2(q_1q_2 + q_3q_0) & 2(q_1q_3 - q_2q_0) \\ 2(q_1q_2 - q_3q_0) & 1 - 2(q_1^2 + q_3^2) & 2(q_2q_3 + q_0q_1) \\ 2(q_1q_3 + q_2q_0) & 2(q_2q_3 - q_1q_0) & 1 - 2(q_1^2 + q_2^2) \end{bmatrix}. \tag{9}$$

The equivalent of a product with a transposed rotation matrix, $\mathbf{u} = M(Q)^T \mathbf{u}_{rot}$, can be written in terms of quaternion multiplications as $\mathbf{u} = Q \otimes \mathbf{u}_{rot} \otimes Q^*$.

If the rotation angle θ is small, the so called error quaternion may be used for the purpose of rotation, and it is obtained by dividing the unit quaternion Q in Eq. 7 by its scalar part [13, 20]:

$$\begin{aligned} Q_v &= \frac{\cos \frac{\theta}{2} + \mathbf{r} \sin \frac{\theta}{2}}{\cos \frac{\theta}{2}} = 1 + \mathbf{r} \tan \frac{\theta}{2} \\ &= [1 \ v_1 \ v_2 \ v_3] = [1 \ \mathbf{v}^T]. \end{aligned} \tag{10}$$

The orientation of a body relative to a fixed frame is usually described in terms of Euler angles. Next we define an operator that relates the Euler angles notation to a unit quaternion description of orientation as

$$\mathcal{T}(\Lambda) = Q = [q_0 \ q_1 \ q_2 \ q_3], \tag{11}$$

where $\Lambda = [\lambda_1 \ \lambda_2 \ \lambda_3]^T$ is a vector of Euler angles, $q_0 = \cos \frac{\lambda_2}{2} \cos \frac{\lambda_1 + \lambda_3}{2}$, $q_1 = \sin \frac{\lambda_2}{2} \cos \frac{\lambda_1 - \lambda_3}{2}$, $q_2 = \sin \frac{\lambda_2}{2} \sin \frac{\lambda_1 - \lambda_3}{2}$ and $q_3 = \cos \frac{\lambda_2}{2} \sin \frac{\lambda_1 + \lambda_3}{2}$ are quaternion elements.

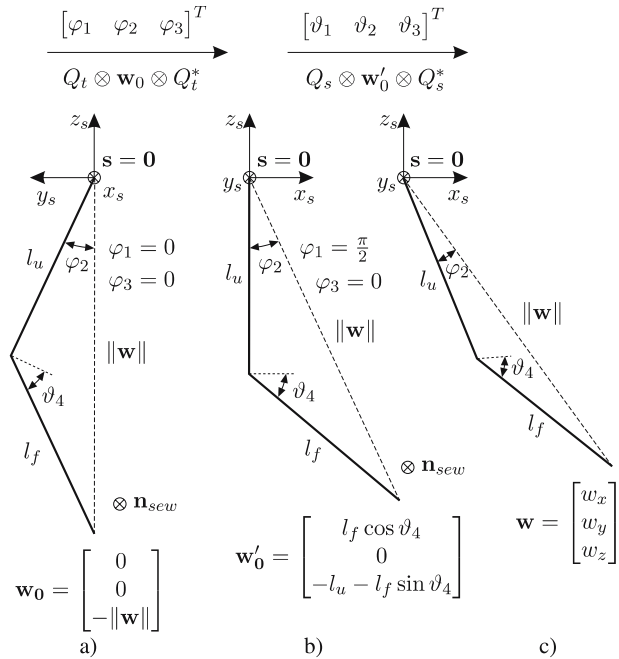
2.4 Quaternion Based Arm Kinematics

The analysis is based on relations in Figure 3. We start with the supposition that the elbow joint angle ϑ_4 represents the only joint variable that affects the distance between the shoulder and the wrist $\|\mathbf{w} - \mathbf{s}\|$. Without losing generality we assume the shoulder position as $\mathbf{s} = [0 \ 0 \ 0]^T$ and consequently $\|\mathbf{w} - \mathbf{s}\| = \|\mathbf{w}\|$. We consider the normal vector of the plane containing the shoulder, elbow and wrist joints, \mathbf{n}_{sew} , parallel to the elbow axis of rotation. Therefore angle ϑ_4 can be estimated trivially using the law of cosines as

$$\vartheta_4 = \arcsin \frac{\|\mathbf{w}\|^2 - l_u^2 - l_f^2}{2l_u l_f}. \tag{12}$$

For the given elbow flexion/extension ϑ_4 we assume the initial position of the wrist exactly below the shoulder joint, $\mathbf{w}_0 = [0 \ 0 \ -\|\mathbf{w}\|]^T$, as in Figure 3a, and the normal

Figure 3 Graphical representation of the shoulder joint rotation sequence from an initial posture (a), through an intermediate posture (b), to the actual arm posture (c).



vector \mathbf{n}_{sew} parallel to the x_s axis. Next we perform a rotation in terms of Euler angles $\Phi = [\varphi_1 \ \varphi_2 \ \varphi_3]^T$, to place the wrist in a position where shoulder angles are $\vartheta_1 = \vartheta_2 = \vartheta_3 = 0$ (see Figure 3b) and

$$\mathbf{w}'_0 = [w'_{0_x} \ w'_{0_y} \ w'_{0_z}]^T = [l_f \cos \vartheta_4 \ 0 \ -l_u - l_f \sin \vartheta_4]^T. \tag{13}$$

The new wrist position is obtained using the following rotations

$$\begin{aligned} \varphi_1 &= \frac{\pi}{2} \\ \varphi_2 &= -\arccos \frac{-w'_{0_z}}{\|\mathbf{w}'_0\|} \\ \varphi_3 &= 0. \end{aligned} \tag{14}$$

The upper arm segment is now parallel to the z_s axis and the normal vector \mathbf{n}_{sew} parallel to the y_s axis. Using the operator (11) we define the quaternion for the above rotation as

$$Q_t = \mathcal{T}(\Phi). \tag{15}$$

The final wrist position $\mathbf{w} = [w_x \ w_y \ w_z]^T$ in Figure 3c can be obtained if actual shoulder angles $\Theta_s = [\vartheta_1 \ \vartheta_2 \ \vartheta_3]^T$ are considered. The rotation can be written in terms of a quaternion as

$$Q_s = \mathcal{T}(\Theta_s). \tag{16}$$

The actual wrist position \mathbf{w} can be obtained as a sequence of two rotations starting from \mathbf{w}_0 as

$$\mathbf{w} = Q_s \otimes Q_t \otimes \mathbf{w}_0 \otimes Q_t^* \otimes Q_s^*. \tag{17}$$

2.5 Estimation Process

We define a vector of available measurements including acceleration data and wrist position as

$$\mathbf{y} = [\mathbf{g}^T \ \mathbf{w}^T]^T \tag{18}$$

and the vector of measurement estimates as

$$\hat{\mathbf{y}} = [\hat{\mathbf{g}}^T \ \hat{\mathbf{w}}^T]^T, \tag{19}$$

with

$$\begin{aligned} \hat{\mathbf{g}} &= \hat{Q}_s^* \mathbf{g}_0 \hat{Q}_s \\ \hat{\mathbf{w}} &= \hat{Q}_s \otimes Q_t \otimes \mathbf{w}_0 \otimes Q_t^* \otimes \hat{Q}_s^*, \end{aligned} \tag{20}$$

where \hat{Q}_s is an estimate of the true attitude quaternion Q_s and $\mathbf{g}_0 = [0 \ 0 \ -g]^T$.

The error between the actual measurement and its estimate is the input signal to the estimation of the new upper arm attitude quaternion. Therefore, we define the estimation error vector as

$$\mathbf{\Upsilon} = \mathbf{y} - \hat{\mathbf{y}}. \tag{21}$$

We begin the estimation process with an initial estimate \hat{Q}_s and use the estimation error vector to calculate the next estimate \hat{Q}_{s+} . The small rotation from the current estimated attitude \hat{Q}_s to the next estimated attitude \hat{Q}_{s+} is defined as an error quaternion Q_v as in Eq. 10. The error quaternion is small but non-zero, due to errors in the various sensors. The relationship is expressed in terms of quaternion multiplication as in [13]

$$\hat{Q}_{s+} = \hat{Q}_s \otimes [1 \ \mathbf{v}^T] = \hat{Q}_s \otimes Q_v. \tag{22}$$

The goal of the estimation process is the minimization of the error vector, therefore we define the cost function as

$$\min f(\mathbf{v}) = \frac{1}{2} \mathbf{\Upsilon}^T \mathbf{\Upsilon}. \tag{23}$$

The Gauss–Newton method may be utilized to minimize the cost function with respect to the variable \mathbf{v} [12, 13]. We define a Jacobian that relates the estimation error vector to the error quaternion as

$$\mathbf{\Upsilon} = -\mathbf{J}(\mathbf{v})\mathbf{v}. \tag{24}$$

The updated error quaternion is then given by

$$Q_v = [1 - ((\mathbf{J}(\mathbf{v})^T \mathbf{J}(\mathbf{v}))^{-1} \mathbf{J}(\mathbf{v})^T \mathbf{\Upsilon})^T], \tag{25}$$

where $(\mathbf{J}(\mathbf{v})^T \mathbf{J}(\mathbf{v}))^{-1} \mathbf{J}(\mathbf{v})^T$ is the Jacobian pseudoinverse. We can now rewrite Eq. 22 as

$$\hat{Q}_{s^+} = \hat{Q}_s \otimes [1 - ((\mathbf{J}(\mathbf{v})^T \mathbf{J}(\mathbf{v}))^{-1} \mathbf{J}(\mathbf{v})^T \boldsymbol{\Upsilon})^T]. \tag{26}$$

In order to compute the Jacobian matrix we use the definition of the vector of measurement estimates (19)

$$\hat{\mathbf{y}}(\hat{Q}_{s^+}) = \begin{bmatrix} \hat{Q}_{s^+}^* \mathbf{g}_0 \hat{Q}_{s^+} \\ \hat{Q}_{s^+} \otimes Q_t \otimes \mathbf{w}_0 \otimes Q_t^* \otimes \hat{Q}_{s^+}^* \end{bmatrix}. \tag{27}$$

Taking into consideration Eqs. 20 and 22, Eq. 27 can be rewritten as

$$\begin{aligned} \hat{\mathbf{y}}(\hat{Q}_{s^+}) &= \begin{bmatrix} (\hat{Q}_s \otimes Q_v)^* \mathbf{g}_0 (\hat{Q}_s \otimes Q_v) \\ (\hat{Q}_s \otimes Q_v) \otimes Q_t \otimes \mathbf{w}_0 \otimes Q_t^* \otimes (\hat{Q}_s \otimes Q_v)^* \end{bmatrix} \\ &= \begin{bmatrix} Q_v^* \otimes \hat{\mathbf{g}} \otimes Q_v \\ (\hat{Q}_s \otimes Q_v \otimes \hat{Q}_s^*) \otimes \hat{\mathbf{w}} \otimes (\hat{Q}_s \otimes \hat{Q}_v^* \otimes Q_s^*) \end{bmatrix}. \end{aligned} \tag{28}$$

Equation 28 expressed in terms of rotation matrices (9)

$$\hat{\mathbf{y}}(\hat{Q}_{s^+}) = \hat{\mathbf{y}}(\mathbf{v}) = \begin{bmatrix} M(Q_v) \hat{\mathbf{g}} \\ M(\hat{Q}_s)^T M(Q_v)^T M(\hat{Q}_s) \hat{\mathbf{w}} \end{bmatrix} \tag{29}$$

can be used for the Jacobian matrix synthesis

$$\begin{aligned} \mathbf{J}(\mathbf{v}) &= - \frac{\partial \hat{\mathbf{y}}(\mathbf{v})}{\partial \mathbf{v}} = - \begin{bmatrix} \frac{\partial \hat{\mathbf{y}}(\mathbf{v})}{\partial v_1} & \frac{\partial \hat{\mathbf{y}}(\mathbf{v})}{\partial v_2} & \frac{\partial \hat{\mathbf{y}}(\mathbf{v})}{\partial v_3} \end{bmatrix} \\ &= - [\mathbf{j}_1(\mathbf{v}) \ \mathbf{j}_2(\mathbf{v}) \ \mathbf{j}_3(\mathbf{v})]. \end{aligned} \tag{30}$$

By evaluating Eq. 30 at $\mathbf{v} = 0$, the column $\mathbf{j}_i(\mathbf{v})$ of the Jacobian matrix $\mathbf{J}(\mathbf{v})$ can be expressed as

$$\mathbf{j}_i(\mathbf{v})|_{\mathbf{v}=0} = \begin{bmatrix} \frac{\partial M(Q_v)}{\partial v_i} |_{\mathbf{v}=0} \hat{\mathbf{g}} \\ M(\hat{Q}_s)^T \frac{\partial M(Q_v)^T}{\partial v_i} |_{\mathbf{v}=0} M(\hat{Q}_s) \hat{\mathbf{w}} \end{bmatrix}. \tag{31}$$

It should be noted that the partial derivative $\frac{\partial M(Q_v)}{\partial v_i} |_{\mathbf{v}=0}$ is a simple constant matrix; for example

$$\frac{\partial M(Q_v)}{\partial v_1} |_{\mathbf{v}=0} = \begin{bmatrix} 0 & 0 & 0 \\ 0 & 0 & 2 \\ 0 & -2 & 0 \end{bmatrix}. \tag{32}$$

2.6 Kalman Filter Formulation

Let the following equation describe a single axis gyroscope model

$$\xi = \omega + b + n_w, \tag{33}$$

where ω is the actual angular rate, b is a bias signal and n_w is the sensor noise. We define a system state vector as

$$\mathbf{x} = \begin{bmatrix} \boldsymbol{\Omega} \\ \mathbf{b} \\ Q_s \end{bmatrix}, \tag{34}$$

where $\boldsymbol{\Omega} = [\omega_x \ \omega_y \ \omega_z]^T$ and $\mathbf{b} = [b_x \ b_y \ b_z]^T$. The derivatives of the state vector \mathbf{x} are as follows:

$$\dot{\mathbf{x}} = \frac{1}{\tau}(\boldsymbol{\Omega} + \mathbf{n}_w), \tag{35}$$

where τ is a time constant and $\mathbf{n}_w = [n_{w_x} \ n_{w_y} \ n_{w_z}]^T$,

$$\dot{\mathbf{b}} = \mathbf{0}^{3 \times 1}, \tag{36}$$

since we expect gyroscope bias to be only slowly varying and the angular rate $\boldsymbol{\Omega}$ and the quaternion derivative \dot{Q}_s are related by the identity [21]

$$\dot{Q}_s = \frac{1}{2}\boldsymbol{\Omega} \otimes Q_s. \tag{37}$$

The quaternion Q_s may be treated as a measurement available to the Kalman filter. Combined with the angular rate measurements, $\Xi = [\xi_x \ \xi_y \ \xi_z]^T$, the Kalman filter has a total of seven measurements. Let $\mathbf{z} = [\Xi^T \ Q_s]^T$ denote the measurement vector. The measurement equation for the Kalman filter is given by

$$\mathbf{z} = \mathbf{G}\mathbf{x} + \mathbf{n}_v, \tag{38}$$

with the noise \mathbf{n}_v and the measurement matrix

$$\mathbf{G} = \begin{bmatrix} \mathbf{I}^{3 \times 3} & \mathbf{I}^{3 \times 3} & \mathbf{0}^{3 \times 4} \\ \mathbf{0}^{4 \times 3} & \mathbf{0}^{4 \times 3} & \mathbf{I}^{4 \times 4} \end{bmatrix}, \tag{39}$$

where \mathbf{I} and $\mathbf{0}$ are unit and zero matrices respectively.

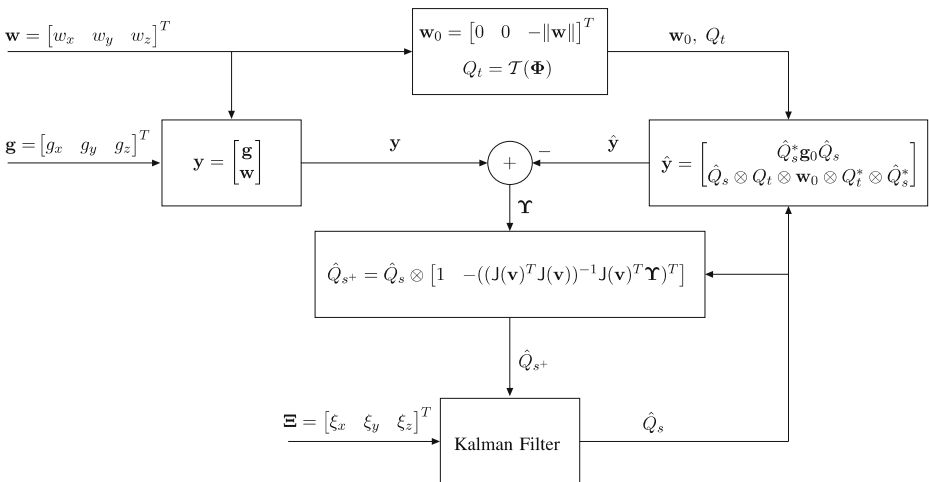


Figure 4 Estimation of the upper arm attitude quaternion Q_s .

A block scheme of the complete estimation process is shown in Figure 4.

2.7 Representation of Arm Posture

The arm posture is represented with three quaternions describing the orientation of the upper arm, the forearm and the hand. The quaternion Q_s (shoulder rotations) is a direct output of the estimation process presented in Sections 2.5 and 2.6. The quaternion Q_e (elbow rotation) describing the orientation of the forearm relative to the upper arm can be computed from Euler angles describing the elbow rotation as

$$Q_e = \mathcal{T} \left(\left[\frac{\pi}{2} \ \vartheta_4 \ -\frac{\pi}{2} \right]^T \right). \quad (40)$$

The hand posture expressed in the base coordinate frame can be determined from the robot kinematic data and its orientation written in a quaternion form as Q_H . The orientation of the hand relative to the forearm can then be computed as

$$Q_w = \mathcal{T} \left([\vartheta_5 \ \vartheta_6 \ \vartheta_7]^T \right) = (Q_s \otimes Q_e)^{-1} \otimes Q_H. \quad (41)$$

3 Experimental Setup

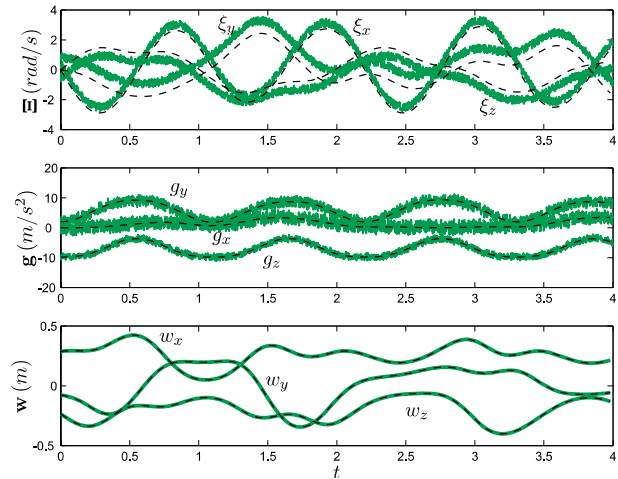
The performance of the system utilizing derived calculation approach was evaluated in a simulation based study and on healthy volunteers. For the simulation based study accelerations and angular rates of the upper arm were calculated from the arm motion. Noisy accelerometer and gyroscope sensor models were applied. Sensor outputs are shown in Figures 5 and 6. Gyroscope signals were corrupted with a bias signal and a uniformly distributed random signal, while accelerometers were distorted only with uniformly distributed random signal. No bias signal was added since accelerometers can easily be calibrated with respect to the Earth gravity field [18]. Wrist position and orientation were supposed to be measured accurately. Therefore, no additional noise was applied.

The inertial measurement system used in experiments consisted of two-axis accelerometers ADXL203 (Analog Device, Inc.) and single-axis gyroscopes ADXRS150 (Analog Device, Inc.). The system was attached on the subject's upper

Figure 5 Experimental setup—robot Staubli RX90B with JR3 force sensor, inertial system attached to the upper arm, and OPTOTRAK infrared markers on the arm, hand, and robot handle.



Figure 6 Simulation based study – available measurement: angular rate, Ξ , acceleration, \mathbf{g} , and wrist position, \mathbf{w} (gray – measured, black – actual).



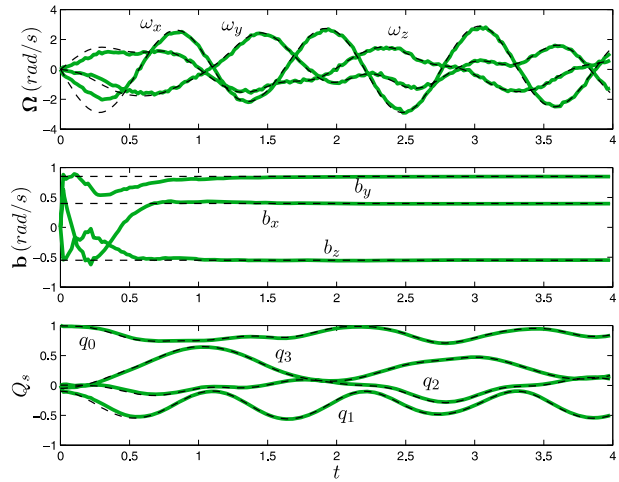
arm using an elastic band. An industrial type robot Staubli RX90B (Staubli Faverges SCA) with a custom designed open architecture controller was used in the evaluation procedure. The robot was programmed to behave like a haptic device and to generate resistance to subject's voluntary arm movements based on a predefined virtual environment. A six axis force/torque sensor (JR3 Inc.) was used for measuring interaction forces between the human and the robot. An admittance type controller running on RTLinux operating system with 4 kHz sampling frequency enabled implementation of a simple virtual environment consisting of an empty box-shaped space with stiff virtual walls. In this way was the subject allowed to move the robot with minimal arm force within the box, while stiff walls prevented the movement outside of the confined space. All signals were sampled at 1 kHz frequency.

Independently were the position and the orientation of the arm and hand measured using the contactless position acquisition system OPTOTRAK (Northern Digital Inc.) with infrared markers that were placed on the shoulder, elbow, and wrist joints as well as on the first joint of the index and the ring fingers. The accuracy of the acquired marker position in space is within ± 0.5 mm. However, the geometry of arm joints, complex shape of arm segments and movement of soft tissue that includes muscles and skin reduce the measuring accuracy of arm joint angles to a degree level.

4 Results

Figure 7 presents the results of the simulation based study, namely the elements of the estimated system state vector \mathbf{x} . It can be observed that after approximately one second the system states are accurately traced. During the first second the estimation errors can mostly be attributed to poor gyroscope bias estimates, \mathbf{b} , which start with the zero initial guess value and have a relatively long setting time (36). Gyroscope bias signal can in general be arbitrarily high and will be accurately estimated. The simulated results show that the estimation process eliminates slowly varying bias component from the gyroscope signal as well as high frequency noise

Figure 7 Simulation based study – elements of system state vector: angular rate, Ω , gyroscope bias, \mathbf{b} , and attitude quaternion, Q_s (gray – estimated, black – actual).



present in accelerometers and gyroscopes. The estimated quaternion Q_s is smooth and accurate.

Experimental results from a measurement session with a healthy subject are presented in Figures 8 and 9. Figure 8 shows the measured upper arm angular velocity vector, Ξ , the upper arm acceleration vector, \mathbf{g} , and the wrist position vector, \mathbf{w} . The average root-mean-square (*rms*) noise of the measured acceleration was $0.5 \cdot 10^{-3} \text{ m/s}^2$ and the average *rms* noise of the measured angular velocity was $0.15 \cdot 10^{-3} \text{ rad/s}$. However, large acceleration and angular velocity spikes were observed at time instances when the virtual wall was hit (see Figure 8). At the same time gyroscope signals contained bias components in the range between -0.03 and 0.02 rad/s . The wrist position, which was measured using the robot joint sensors was found very accurate and contained negligible noise.

Figure 8 Available measurement: angular rate, Ξ , acceleration, \mathbf{g} , and wrist position, \mathbf{w} (gray – estimated, black – from optical measurement system).

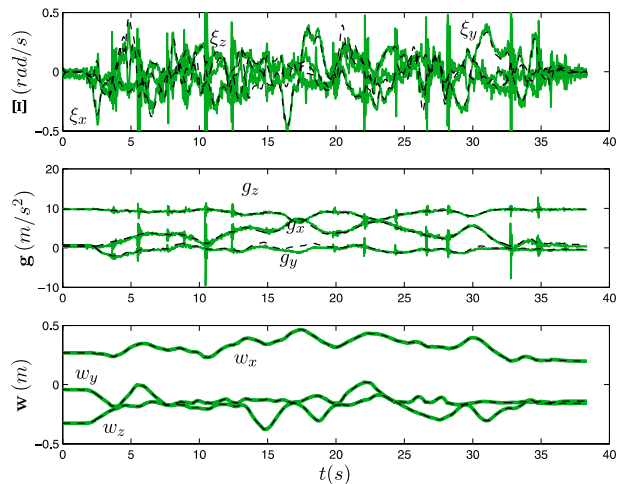


Figure 9 Attitude quaternions for shoulder, Q_s , elbow, Q_e , and wrist, Q_w (gray – estimated, black – from optical measurement system).

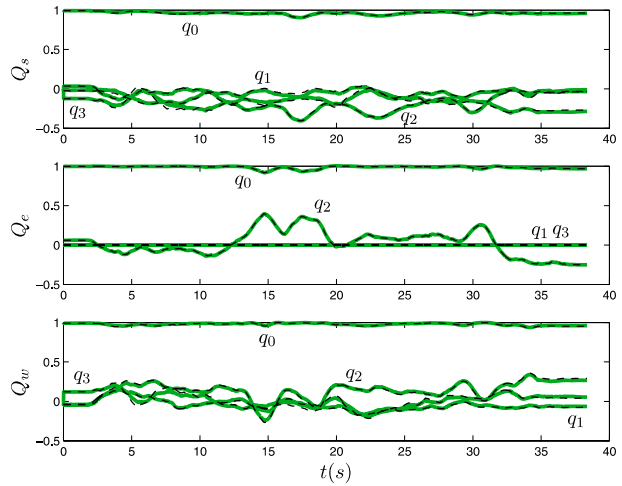


Figure 9 shows the estimated attitude quaternions describing the orientation of the upper arm, forearm and the hand. Despite the noisy signals generated by the gyroscopes and accelerometers, the estimated quaternions are practically noiseless (noise *rms* below 10^{-5}). Neither sensor noise nor spikes resulting from the collisions with the virtual walls do not affect the estimation process. The difference between the arm posture estimated from the optical measurement system and the posture estimated using the inertial system was found within the accuracy limits of the optical measurement system for all feasible robot and human arm postures.

A detailed analysis indicates that the estimation process is robust to sensor noise present in the accelerometers and gyroscopes. Gyroscope bias signal estimation error was below $0.5 \cdot 10^{-3}$ rad/s. On the other hand, the system performance is sensitive to the wrist position measurements, because there is no redundancy in the data. However, since the robot end-effector position is usually accurately measured, this is not a problematic issue.

5 Summary and Conclusions

The paper depicts a technique for computation of the inverse kinematic model of the human arm using a quaternion description. The approach is based on measurements of the hand position and orientation as well as acceleration and angular rate of the upper arm segment. The algorithm is simple and numerically robust. It generates accurate estimates of human arm posture, regardless of the noise present in the sensors. Results can be applied in robot trajectory planning for rehabilitation purposes, for evaluation of movement capabilities of patients with movement disorders and in control algorithms for artificial activation of upper extremity muscles using functional electrical stimulation or exoskeleton devices.

One of the limiting factor in the implementation of the inverse kinematics algorithm is the required fixation of the shoulder joint. However, having in mind that the subject is usually sited during upper extremity rehabilitation, the fixation of the shoulder joint can simply be accomplished by using belts that are attached to the back

of the chair. The correctness of the supposition was also validated experimentally. Namely, the accuracy of measurements presented in Section 4 was achieved with the subject sitting on a chair without a backrest and without any other shoulder fixation.

Acknowledgements This work was supported by the Ministry of Education, Science and Sport of the Republic of Slovenia.

References

1. Tejima, N.: Rehabilitation robotics: a review. *Adv. Robot.* **14**, 551–564 (2000)
2. Lenarčič, J., Klopčar, N.: Positional kinematics of humanoid arms. *Robotica* **24**, 105–112 (2006)
3. Korein, J.: A geometric investigation of reach. Ph.D. Dissertation, University of Pennsylvania (1985)
4. Tolani, D., Badler, N.I.: Real-time inverse kinematics of the human arm. *Presence* **5**, 393–401 (1996)
5. Koga, Y., Kondo, K., Kuffner, J., Latombe, J.: Planning motions with intentions. In: Proc., SIGGRAPH'94, Orlando, Florida, July 24–29, pp. 395–407 (1994)
6. Soechting, J.F., Flanders, M.: Sensorimotor representations for pointing to targets in three dimensional space. *J. Neurophysiol.* **62**, 582–594 (1989)
7. Loftin, R.B., Maida, J.C., Yang, J.: Inverse kinematics of the human arm. Technical report, The University of Houston, Texas (1997)
8. Tsiotras, P., Longuski, J.M.: A new parametrization of the attitude kinematics. *J. Astronaut. Sci.* **43**, 243–263 (1995)
9. Spring, K.W.: Euler parameters and the use of quaternion algebra in the manipulation of finite rotations: a review. *Mech. Mach. Theory* **21**, 365–373 (1986)
10. Shuster, M.D.: A survey of attitude representations. *J. Astronaut. Sci.* **41**, 439–517 (1993)
11. Chou, J.C.K.: Quaternion kinematic and dynamic differential equations. *IEEE Trans. Robot. Autom.* **8**, 53–64 (1992)
12. Marins, J.L., Yun, X., Bachmann, E.R., McGhee, R.B., Zyda, M.J.: An extended kalman filter for quaternion-based orientation estimation using marg sensors. In: Proceedings of the 2001 IEEE/RSJ International Conference on Intelligent Robots and Systems, Maui, Hawaii, pp. 2003–2011 (2001)
13. Yun, X., Lizaraga, M., Bachmann, E.R., McGhee, R.B.: An improved quaternion-based kalman filter for real-time tracking of rigid body orientation. In: Proceedings of the 2003 IEEE/RSJ International Conference on Intelligent Robots and Systems, Las Vegas, Nevada, pp. 1074–1079 (2003)
14. Kong, X.: INS algorithm using quaternion model for low cost IMU. *Robot. Auton. Syst.* **46**, 221–246 (2004)
15. Natale, C.: *Interaction Control of Robot Manipulators*. Springer, Berlin Heidelberg New York (2003)
16. Stavadahl, O., Bondhus, A.K., Pettersen, K.Y., Malvig, K.E.: Optimal statistical operators for 3-dimensional rotational data: Geometric interpretations and application to prosthesis kinematics. *Robotica* **23**, 283–292 (2005)
17. Tolani, D., Goswami, A., Badler, N.I.: Real-time inverse kinematics techniques for anthropomorphic limbs. *Graph. Models* **62**, 353–388 (2000)
18. Lee, J., Ha, I.: Sensor fusion and calibration for motion captures using accelerometers. In: Proceedings of the 1999 IEEE International Conference on Robotics & Automation, Detroit, Michigan, pp. 1954–1959 (1999)
19. Mihelj, M., Munič, M.: Estimation of human arm angles using hand pose data and upper arm radial acceleration measurements. In: Proceedings, 8th International Conference on Rehabilitation Robotics, Daejeon, Korea, pp. 302–305 (2003)
20. Ang, D.G.-E., Elkaim, G.H., Powell, J.D., Parkinson, B.W.: A gyro-free quaternion based attitude determination system suitable for implementation using low cost sensors. In: Proceedings of IEEE 2000 Position Location and Navigation Symposium, San Diego, California, pp. 185–192 (2000)
21. Kuipers, J.B.: *Quaternions and Rotation Sequences*. Addison-Wesley, Reading, Massachusetts, (1999)